

Efficient pseudo-random number generators for biomolecular simulations on graphics processors

A. Zhmurov^{1,2}, K. Rybnikov³, Y. Kholodov¹ and V. Barsegov^{2,1*}

¹*Moscow Institute of Physics and Technology, Dolgoprudnyi, Moscow region, Russia, 141700*, ²*Department of Chemistry and* ³*Department of Mathematics, University of Massachusetts, Lowell, MA 01854*

(Dated: November 6, 2018)

Langevin Dynamics, Monte Carlo, and all-atom Molecular Dynamics simulations in implicit solvent, widely used to access the microscopic transitions in biomolecules, require a reliable source of random numbers. Here we present the two main approaches for implementation of random number generators (RNGs) on a GPU, which enable one to generate random numbers on the fly. In the one-RNG-per-thread approach, inherent in CPU-based calculations, one RNG produces a stream of random numbers in each thread of execution, whereas the one-RNG-for-all-threads approach builds on the ability of different threads to communicate, thus, sharing random seeds across the entire GPU device. We exemplify the use of these approaches through the development of Ran2, Hybrid Taus, and Lagged Fibonacci algorithms fully implemented on the GPU. As an application-based test of randomness, we carry out LD simulations of N independent harmonic oscillators coupled to a stochastic thermostat. This model allows us to assess statistical quality of random numbers by comparing the simulation output with the exact results that would be obtained with truly random numbers. We also profile the performance of these generators in terms of the computational time, memory usage, and the speedup factor (CPU/GPU time).

arXiv:1003.1123v1 [physics.chem-ph] 4 Mar 2010

*Corresponding author; phone: 978-934-3661; fax: 978-934-3013; Valeri_Barsegov@uml.edu

I. INTRODUCTION

Over the last few years, graphics processors have evolved into highly parallel, multithreaded computing devices. Graphics Processing Units (GPUs) are now emerging as an alternative programming platform that provides high raw computational power for scientific applications [1–8]. Because GPUs implement Single Instruction Multiple Data (SIMD) architecture with reduced cache and flow control for a group of computational cores, most of a GPU device form computational units dedicated to actual calculations. The computational efficiency of contemporary GPUs can reach striking 1 TFlops for a single chip [9], the number not yet accessible even for most up-to-date CPUs. With introduction of CUDA (Compute Unified Device Architecture) by NVIDIA (a dialect of C and C++ programming languages) [9, 10], GPUs have become capable of performing compute-intensive scientific calculations. Because the GPU-based calculations are 10–50 times faster than some of the heavily tuned CPU-based methods, GPUs are being used as performance accelerators in a variety of applications [1, 2, 7, 8].

The GPU-based calculations can be performed concurrently on many computational cores, called Arithmetic Logic Units (ALUs), that are grouped into multiprocessors, each with its own flow control and cache units. For example, in contemporary graphics cards from NVIDIA each multiprocessor contains up to eight $\sim 1.3GHz$ ALUs and 14–16KB of cache (8KB of constant memory cache and 6–8KB of the global memory cache when accessed through texture references). The number of multiprocessors per GPU can reach 30 on the most up-to-date graphics cards (Tesla C1060 or GeForce GTX 285), thus, bringing the total number of ALUs to 240 per chip. Due to the inherently parallel nature of the GPU-based calculations, achieving optimal performance on the GPU mandates that a computational task be divided into many independent threads of execution that run in parallel performing the same operation but on different data sets. Although each graphics card has its own global memory with ~ 10 times larger bandwidth compared to DRAM on a CPU, the number of memory invocations (per ALU) should be minimized to optimize the GPU performance. Hence, the computational task should be compute-intensive so that, most of the time, the GPU is busy performing computations rather than reading and writing data [9, 10]. This makes a classical N body problem that would be difficult or impossible to solve exactly into a prime candidate for the numerical implementation on the GPU.

Computer simulations of a system of N particles, e.g., Langevin Dynamics (LD), Monte Carlo (MC), and Molecular Dynamics (MD) simulations, are among many applications that can be implemented on the GPU. In LD and MD simulations, atomic interactions are described by

the same potential energy function (force field) applied to all particles in the system. Hence, there is a direct mapping between the SIMD architecture of the GPU (hardware) and numerical routines (software) used to follow a trajectory of the system under the study in real time. In a sense, a “single instruction”, i.e. calculation of the potential energy terms or evaluation of forces and random forces, or numerical integration of the equation(s) of motion, is executed on “multiple data” sets (for all particles) in order to describe the dynamics of the whole system. For example, in MD simulations of biomolecules in implicit solvent (water) [11, 12], the dynamics of the i -th particle are governed by the equations of motion for the particle position, $d\mathbf{R}_i/dt=\mathbf{V}_i$ ($\mathbf{R}_i=\{R_{i,x}, R_{i,y}, R_{i,z}\}$), and velocity, $m_i d\mathbf{V}_i/dt=\xi\mathbf{V}_i+\mathbf{f}(\mathbf{R}_i)+\mathbf{G}_i(t)$ ($\mathbf{V}_i=\{V_{i,x}, V_{i,y}, V_{i,z}\}$), where m_i is the particle mass, ξ is the friction coefficient, $\mathbf{f}(\mathbf{R}_i) = -\partial\mathbf{U}/\partial\mathbf{R}_i$ is the molecular force exerted on the i -th particle due to the potential energy $\mathbf{U}=\mathbf{U}(\mathbf{R}_1, \mathbf{R}_2, \dots, \mathbf{R}_N)$, and $\mathbf{G}_i(t)=\{G_{i,x}, G_{i,y}, G_{i,z}\}$ is the Gaussian random force with the first moment $\langle\mathbf{G}_i(t)\rangle=0$ and the two-point correlation function $\langle\mathbf{G}_i(t)\mathbf{G}_j(t')\rangle = 2k_B T \xi \delta_{ij} \delta(t-t')$ ($i, j=1, 2, \dots, N$) [13]. In LD simulations of proteins, the dynamics of the i -th C_α -particle is governed by the Langevin equation for \mathbf{R}_i , $\xi d\mathbf{R}_i/dt=\mathbf{f}(\mathbf{R}_i)+\mathbf{G}_i(t)$ [14]. These equations of motion are solved numerically over many iterations of the simulation algorithm.

Since in MD simulations in implicit water and in LD simulations, the effect of solvent molecules is described implicitly, these methods require a reliable source of $3N$ normally distributed random numbers, $g_{i,\alpha}$ ($i=1, 2, \dots, N$) to compute the components of the Gaussian random force $G_{i,\alpha}=g_{i,\alpha}\sqrt{2k_B T \xi \Delta t}$, where Δt is the time step ($\alpha=x, y, \text{ and } z$). In MC simulations, the results of multiple independent trials, each driven by some random process, are combined to extract the average answer. A pseudo-random number generator, or algorithmic RNG, must have a long period and must meet the conflicting goals of being fast while also providing a large amount of random numbers of proven statistical quality [15]. An RNG produces a deterministic sequence of random numbers, u_i , that are supposed to imitate realizations of independent uniform random variables from the interval $(0, 1)$, i.e., i.i.d. $U(0, 1)$. This sequence (u_i) is translated into the sequence of normally distributed random variables (g_i) using the ziggurat method [16] or the polar method [17], or the Box-Mueller transformation [18]. There is an extensive body of literature devoted to random number generation on the CPU [19]. Yet, due to fundamental differences in processor and memory architecture of CPU and GPU devices, the CPU-based methods cannot be easily translated from the CPU to the GPU. While there exist stand-alone implementations of good quality RNGs on the GPU, to fully utilize computational resources of the GPU in molecular simulations an RNG should be incorporated into the main simulation program. This enables a developer to minimize read/write calls associated with invocation of

the relatively slow GPU global memory, and to generate streams of random numbers using fast GPU shared memory.

We present a novel methodology for generating pseudo-random numbers on a GPU on the fly, i.e. at each step of a simulation run. This methodology can be used in the development of the GPU-based implementations of MD simulations in implicit solvent, and in LD and MC simulations. We focus on the Linear Congruential Generator (LCG), and the Ran2, Hybrid Taus, and Lagged Fibonacci algorithms reviewed in the next Section. These algorithms are used in Section III to describe the one-RNG-per-thread approach and the one-RNG-for-all-threads approach for random number generation on the GPU. In the one-RNG-per-thread setting, one RNG is assigned for each computational thread (for each particle), a procedure commonly used in the CPU-based calculations. The one-RNG-for-all-threads method utilizes the ability of different threads to communicate across the entire GPU device (pseudocodes are given in the Appendices). We test the performance of GPU-based implementations of these generators in Section IV, where we present application-based assessment of their statistical qualities using Langevin simulations of N independent Brownian particles evolving on the harmonic potential. We profile these generators in terms of the computational time and memory usage for varying system size N . The main results are discussed in Section V, where we provide recommendations on the use of RNG algorithms.

II. PSEUDORANDOM NUMBER GENERATORS

A. Overview

There are three types of random numbers generators: true or hardware random numbers generators, and software-based quasi-random numbers generators and pseudo-random numbers generators (RNGs) [20]. In this paper we focus on algorithmic RNGs - the most common type of deterministic random number generators. Because an RNG produces a sequence of random numbers in a purely deterministic fashion, a good quality RNG should have a long period and should pass some stringent statistical tests for uniformity and independence. MD simulations of biomolecules in implicit water and LD simulations of proteins use normally distributed random forces to emulate stochastic kicks from the solvent molecules. To generate the distribution of random forces, a common approach is to convert the uniformly distributed random variates into the Gaussian distributed random variates using a particular transformation. In this paper, we adopt the most commonly used Box-Mueller transformation [18].

There are three main requirements for a numerical implementation of an RNG: (1) good statistical properties, (2) high computational speed, and (3) low memory usage. A deterministic sequence of random numbers comes eventually to a starting point, i.e. to the initial set of random seeds $u_{n+p}=u_n$ [21]. This mandates that an RNG should have a long period p . For example, a simulation run might use 10^{12} random numbers, in which case the period must far exceed 10^{12} . Once an RNG has been selected and implemented, it must also be tested empirically for randomness, i.e., for the uniformity of distribution and for the independence [15]. In addition, it must also pass application-based tests of randomness that offer exact solutions to the test applications. Using random numbers of poor statistical quality in molecular simulations might result in insufficient sampling, unphysical correlations or even patterns [22, 23], and unrealistic results, which leads to errors in practical applications [24]. Some of the statistical tests of randomness are accumulated in the DIEHARD test suite and in the TestU01 library [15, 25–27]. In numerical implementations, a good quality RNG should also be computationally efficient so that random number generation does not become a major bottleneck. For example, in LD simulations of proteins on a GPU, one can obtain long 0.1s trajectories over as many as 10^{10} iterations. Hence, to simulate one trajectory for a system of 10^3 particles requires total of $\sim 10^{13}$ random numbers. The requirement of low memory usage is also important as modern graphics processors have low on-chip memory, $\sim 20KB$ per multiprocessor, compared to $\sim 2MB$ memory on the CPU. Hence, an efficient RNG algorithm must use limited working area without invoking the slow GPU global memory.

Typically, a fast RNG employs simple logic and a few state variables to store its current state, but this may harm statistical properties of the random numbers produced. On the other hand, using more sophisticated algorithms with many arithmetic operations or combining several generators into a hybrid generator allows to improve statistics, but these generators are slower and use more memory. Hence, a choice of RNG is determined primarily by specific needs of a particular application, including statistical characteristics of random numbers, and GPU capabilities. In this paper, we focus on the most widely used algorithms: Linear Congruential Generator (LCG) [19], and the Ran2 [19], Hybrid Taus generator [19, 20, 28, 29] and Lagged Fibonacci algorithm [19, 30, 31]. LCG can be used in performance benchmarks since it employs a very fast algorithm. Ran2 is a standard choice for MD simulations of biomolecules in implicit water and in LD simulations of proteins due to its long period ($p > 2 \times 10^{18}$), good statistical quality, and high computational performance on the CPU. However, Ran2 requires large amount of on-chip GPU local memory and global memory to store its current state. Hybrid Taus is an example of how several simple algorithms can be combined to improve statistical characteristics

of random numbers. It scores better in terms of the computational speed on the GPU than KISS, the best known combined generator [32], and its long period ($p > 2 \times 10^{36}$) makes it a good choice for molecular simulations on the GPU. Lagged Fibonacci employs very simple logic while producing random numbers of high statistical quality [15, 31]. It is commonly used in distributed MC simulations, and it can also be utilized in GPU-based computations. Here, we briefly review the LCG, Ran2, Hybrid Taus, and Lagged Fibonacci algorithms.

B. Linear Congruential Generator

The Linear Congruential Generators (LCGs) are the classic and most popular class of generators, which use a transitional formula,

$$x_n = (ax_{n-1} + c) \bmod m, \quad (1)$$

where m is the maximum period, and $a=1664525$ and $c=1013904223$ are constant parameters [19]. To produce a uniformly distributed random number, x_n is divided by 2^{32} . Assuming a 32-bit integer, the maximum period can be at most $p=2^{32}$, which is far too low. LCGs also have known statistical flows [15]. If $m=2^{32}$, one can neglect $\bmod m$ operation as the returned value is low-order 32 bits of the true 64-bit product. Then, the transitional formula reads $x_n=ax_{n-1}+c$, which is the so-called Quick and Dirty (or ranqd2) generator (simplified LCG generator). Quick and Dirty LCG is a very fast generator as it takes only a single multiplication and a single addition to produce a random number, and it uses a single integer to describe its current state. Due to low memory usage, Quick and Dirty LCG can be used to benchmark GPU-based implementations of software packages at the development stage.

C. Ran2

Ran2, one of the most popular RNGs, combines two LCGs and employs randomization using some shuffling procedure [19]. Ran2 has a long period and provides random numbers of very good statistical properties [15]. In fact, Ran2 is one of a very few generators that does not fail a single known statistical test. It is reasonably fast, but there are several features that make Ran2 less attractive for GPU-based computations. First, the algorithm involves long integer arithmetic (64-bit logic) - a computational bottleneck for contemporary GPUs. Secondly, it requires a large amount of memory to store its current state that needs to be updated at each step. This involves a large number of memory calls, which may, potentially, slow down the computational speed on the low cache GPU.

D. Hybrid Taus

Hybrid Taus [20] is a combined generator that uses LCG and Tausworthe algorithms. Tausworthe taus88 is a fast equidistributed modulo 2 generator [28, 29], which produces random numbers by generating a sequence of bits from a linear recurrence modulo 2, and forming the resulting number by taking a block of successive bits. In the space of binary vectors, the n -th element of a vector is constructed using the linear transformation,

$$y_n = a_1 y_{n-1} + a_2 y_{n-2} + \dots + a_k y_{n-k}, \quad (2)$$

where a_n are constant coefficients. Given initial values, y_0, y_1, \dots, y_{n-1} , the n -th random integer is obtained as $x_n = \sum_{j=1}^L y_{ns+j-1} 2^{-j}$, where s is a positive integers and $L=32$ is the integer size (machine word size). Computing x_n involves performing s steps of the recurrence, which might be costly computationally. Fast implementation can be achieved for a certain choice of parameters. When $a_k = a_q = a_0 = 1$, where $0 < 2q < k$ and $a_n = 0$ for $0 < s \leq k - q < k \leq L$, the algorithm can be simplified to a series of binary operations [29]. Statistical characteristics of random numbers produced using taus88 alone are poor, but combining taus88 with LCG removes all the statistical defects [20]. In general, statistical properties of a combined generator are better than those of components. When periods of all components are co-prime numbers, a period of a combined generator is the product of periods of all components. A similar approach is used in the KISS generator, which combines LCG, Tausworthe generator, and a pair of multiple-with-carry generators [32]. However, multiple 32-bit multiplications, used in KISS, may harm performance on the GPU. The period is the lowest common multiplier of the periods of three Tausworthe steps and one LCG. We used parameters that result in periods of $p_1 = 2^{31} - 1$, $p_2 = 2^{30} - 1$, and $p_3 = 2^{28} - 1$ for the Tausworthe generators and a period of $p_4 = 2^{32}$ for the LCG, which makes the period of the combined generator equal $\sim 2^{121} > 10^{36}$. Hybrid Taus uses small memory area since only four integers are needed to store its current state.

E. Lagged Fibonacci

The Lagged Fibonacci algorithm is defined by the recursive relation,

$$x_n = f(x_{n-sl}, x_{n-ll}) \bmod m, \quad (3)$$

where sl and ll are the short and long lags, respectively ($ll > sl$), m defines the maximum period and f is a function that takes two integers x_{n-sl} and x_{n-ll} to produce integer x_n . The most

commonly used functions are multiplication, $f(x_{n-sl}, x_{n-ll})=x_{n-sl}*x_{n-ll}$ (multiplicative Lagged Fibonacci), and addition, $f(x_{n-sl}, x_{n-ll})=x_{n-sl}+x_{n-ll}$ (additive Lagged Fibonacci). Random numbers are generated from the initial set of ll integer seeds, and to achieve the maximum period $\sim 2^{ll-1} \times m$ the long lag ll should be set equal the base of a Mersenne exponent, and the short lag sl should be taken so that the characteristic polynomial $x^{ll}+x^{sl}+1$ is primitive. In addition, sl should not be too small or too close to ll ; it is recommended that $sl \approx \rho \times ll$, where $\rho \approx 0.618$ [31]. When single precision arithmetic is used, the mod m operation can be omitted by setting $m=2^{32}$ (more on selection of parameters can be found in Ref. [31, 33]). We employed the additive Lagged Fibonacci RNG, which generates floating point variates directly, without the usual floating of random integers. Also, sl and ll can be taken to be very large, which improves statistical quality of the generator.

III. GPU-BASED IMPLEMENTATION OF LCG, RAN2, HYBRID TAUS, AND LAGGED FIBONACCI ALGORITHMS

A. Basic ideas

The main feature that makes GPUs computationally efficient is their many-thread architecture, i.e. calculations are performed on a GPU using threads working in parallel. Hence, in molecular simulations of an N body system on a GPU an RNG should produce independent random numbers simultaneously for all particles. One possibility is to have random numbers pre-generated on a CPU or on a GPU, and then use these numbers in simulations. However, this requires a large amount of memory allocated for an RNG. For example, for a system of 10^4 particles in three dimensions, 3×10^4 random numbers are needed at each simulation step. If these numbers are pre-generated, say, for every 100–1000 steps, it requires 3×10^6 – 3×10^7 random numbers to be stored on the GPU, which takes 12–120MB of memory. This might be significant for graphics cards with limited memory, e.g., GeForce GTX 200 series (from NVIDIA) with $\sim 1GB$ of memory. Another approach is to build an RNG into the main simulation kernel. This allows one to achieve top performance for an RNG by maximizing the amount of computations on a GPU while also minimizing the number of calls of the GPU global memory (read/write operations). In addition, to fully utilize the GPU resources, the total number of threads should be ~ 10 -times larger than the number of computational cores, so that none of the cores awaits for the others to complete their tasks.

To develop parallelized implementations of several different RNGs on the GPU, we employ

cycle division paradigm [30]. The idea is to partition a single RNG sequence, which can be viewed as a periodic circle of random numbers, among many computational threads running concurrently across the entire GPU device, each producing a stream of random numbers. Since most RNG algorithms are based on sequential transformations of the current state, including LCG, Hybrid Taus and Ran2, the most common way of partitioning the sequence is to provide each thread with different seeds while also separating the threads along the sequence to avoid possible inter-stream correlations. This is the basis of the one-RNG-per-thread approach (Fig. 1). Also, there exist RNG, e.g., Mersenne Twister and Lagged Fibonacci algorithms, that allow one to leap ahead in the sequence to produce the $(n+1)$ random number without first computing the n -th number [30, 32, 34]. The leap size, which, in general, depends on parameters of an RNG, can be adjusted to the number of threads (equal the number of particles N), or multiples of N ($M \times N$). Then, all N random numbers can be obtained simultaneously, i.e. the j -th thread produces numbers $j, j+N, j+2N \dots$, etc. Note that at the end of each simulation step, threads must be synchronized so that the current RNG state is properly updated. The same RNG state is used by all threads, each updating just one elements of the state. We refer to this as the one-RNG-for-all-threads approach (Fig. 1). In what follows, we describe these approaches in more detail.

B. One-RNG-per-thread approach

The idea is to run the same RNG algorithm in many threads, where all RNGs generate different subsequences of the same sequence of random numbers using the same algorithm, but starting from different initial seeds. First, a CPU generates N sets of random seeds (one for each RNG) and passes them to the GPU global memory (Fig. 2). To exclude correlations, these sets should come from an independent sequence of random numbers, or should be generated using different RNG algorithms on the CPU. In a simulation run, each thread on the GPU reads its random seeds from the GPU global memory and copies them to the GPU local (per thread) memory or shared (per thread block) memory. Then, each RNG can generate as many random numbers as needed, without using the slow GPU global memory. At the end of a simulation step, each RNG saves its current state to the global memory and frees shared memory. Since each thread has its own RNG, there is no need for threads synchronization; however, when particles interact threads must be synchronized. In molecular simulations of a system of N particles, $4N$ uniformly distributed random variates are needed at each step, and arrays of initial seeds and the current state should be arranged for coalescent memory read to speedup the global memory

access. In the one-RNG-per-thread setting, an RNG should be very light in terms of memory usage. Small size of on-chip memory can be insufficient to store the current state of an RNG that is based on a complex algorithm. These restrictions make it difficult to use simple RNG algorithms, especially when statistical properties of random numbers become an issue.

In the one-RNG-per-thread approach, the amount of memory required to store the current state of a generator is proportional to the number of threads (number of particles N). Hence a significant amount of memory has to be allocated for all RNGs to describe the dynamics for a large system. For example, LCG uses one integer seed to store its current state, which takes 4 bytes per thread (per generator) or $\sim 4MB$ of memory for 10^6 threads, whereas Hybrid Taus uses 4 integers, i.e. $16MB$ of memory. These are acceptable numbers, given hundreds of megabytes of the GPU memory. By contrast, Ran2 uses 35 long integers and a total of 280 bytes per thread, or $\sim 280MB$ of memory (for 10^6 threads). As a result, not all seeds can be stored in on-chip (local or shared) memory ($\sim 16KB$), and the Ran2 RNG has to access the GPU global memory to read and update its current state. In addition, less memory becomes accessible to other computational routines. This might prevent using Ran2 in the simulations of large systems on some graphics cards, including GeForce GTX 280 and GTX 295 (NVIDIA), with $768MB$ of global memory (per GPU). However, this is not an issue when using high end graphics cards, such as Tesla C1060 with $4GB$ of global memory. In this paper, we utilized the one-RNG-per-thread approach to develop the GPU-based implementations of the Hybrid Taus and Ran2 algorithms (pseudocodes are presented in Appendix A).

C. One-RNG-for-all-threads approach

Within the one-RNG-for-all-threads approach, one can use a single RNG by allowing all computational threads to share the state of a generator. This approach can be adapted to RNG algorithms that are based on the recursive transformations, i.e., $x_n = f(y_{n-r}, y_{n-r+1}, \dots, y_{n-k})$, where r is the recurrence degree and $k > r$ is a constant parameter. This transformation allows one to obtain a random number at the n -th step from the state variables generated at the previous steps $n-r, n-r+1, \dots, n-k$. If a sequence of random numbers is obtained simultaneously in N threads, each generating just one random number at each step, then total of N random numbers are produced. Then, given $k > N$, all the elements of the transformation have been obtained in the previous steps, in which case they can be accessed without threads synchronization. One of the algorithms that can be implemented on the GPU using the one-RNG-for-all-threads approach is Lagged Fibonacci (Fig. 3) [34]. When one random number is computed in each thread and

when $sl > N$ and $ll - sl > N$ (Section II E), N random numbers can be obtained simultaneously on the GPU without threads synchronization.

To initialize the Lagged Fibonacci RNG on the GPU, ll integers are allocated on the CPU using initial seeds. Each thread then reads two integers from this sequence, which correspond to the long lag ll and the short lag sl , generates the resulting integer, and saves it to the location in the GPU global memory, which corresponds to the long lag. Setting $sl > N$ and $ll - sl > N$ guarantees that the same position in the array of integers (current state variables) will not be accessed by different threads at the same time. The moving window of N random numbers, updated by N threads at each step, is circling along the array of state variables, leaping forward by N positions (at each step). Importantly, a period of the Lagged Fibonacci generator, $p \sim 2^{ll+31}$, can be adjusted to the system size by assigning large values to sl and ll , so that $p \gg N \times S$, where S is the total number of simulation steps. Changing ll and sl does not influence the execution time, but affects the size of the array of state variables, which scales linearly with ll - the amount of integers stored in the GPU global memory. Large ll is not an issue even when $ll \sim 10^6$, which corresponds to $\sim 4MB$ of the GPU global memory (pseudocode for the Lagged Fibonacci RNG is presented in Appendix B). Note, that the GPU-based implementation of the Lagged Fibonacci algorithm using the one-RNG-per-thread approach requires to store N independent RNG states of size ll , i.e. N times larger memory.

IV. APPLICATION-BASED TEST OF RANDOMNESS: ORNSTEIN-UHLENBECK PROCESS

To assess the computational and statistical performance of the LCG, Ran2, Hybrid Taus, and Lagged Fibonacci algorithms in molecular simulations, we carried out Langevin simulations of N independent one-dimensional harmonic oscillators in a stochastic thermostat, fully implemented on the GPU. Each particle evolves on the harmonic potential, $V(R_i) = k_{sp} R_i^2 / 2$, where R_i is the i -th particle position and k_{sp} is the spring constant. We employed this analytically tractable model from statistical physics to compare the results of simulations with the theoretical results that would be obtained with truly random numbers. In the test simulations, we used NVIDIA graphics card GeForce GTX 295, which has two processing units (GPUs), each with 30 multiprocessors (total of 240 ALUs) [9] and 768MB of global memory.

The Langevin equations of motion in the overdamped limit,

$$\xi \frac{dR_i}{dt} = -\frac{\partial V(R_1, R_2, \dots, R_N)}{\partial R_i} + G_i(t), \quad (4)$$

were integrated numerically using the first-order integration scheme (in powers of the integration time step Δt) [35],

$$R_i(t + \Delta t) = R_i(t) + f(R_i(t))\Delta t/\xi + g_i(t)\sqrt{2k_B T\xi\Delta t}, \quad (5)$$

where $f(R_i) = -(\partial V(R_1, R_2, \dots, R_N)/\partial R_i)$ is the force acting on the i -th oscillator [36–38]. In Eq. (5), g_i are the Gaussian distributed random variates (with zero mean and unit variance), which are transformed into the random forces $G_i(t) = g_i(t)\sqrt{2k_B T\xi\Delta t}$. Langevin dynamics in the overdamped limit (Eqs. (4) and (5)) are widely used in the simulations of biomolecules [37–43]. Numerical values of the constant parameters for the LCG, Ran2, Hybrid Taus, and Lagged Fibonacci algorithms can be found, respectively, in Section II [15], in Ref. [19], in Appendix A, and in Table I.

We employed the one-RNG-per-thread approach to develop the GPU-based implementations of the LCG, Ran2, and Hybrid Taus algorithms, and used the one-RNG-for-all-threads approach for the Lagged Fibonacci RNG. These implementations have been incorporated into the LD simulation program written in CUDA. Numerical algorithms for the GPU-based implementation of LD simulations of biomolecules, which involves evaluation of the potential energy, calculation of forces, and numerical integration of the Langevin equations of motion, will be presented in a separate publication (A. Zhmurov, R. I. Dima, Y. Kholodov, and V. Barsegov, submitted to *J. Chem. Theory and Comput.*) In our implementation, each computational thread generates one trajectory for each particle, and we used 64 threads in a thread block. Numerical calculations for $N=10^4$ particles were carried out with the time step $\Delta t=1ps$, starting from the initial position $R_0=10nm$, and using $k_{sp}=0.01pN/nm$, $T = 300K$, and $D = 0.25nm^2/ns$. Soft harmonic spring ($0.01pN/nm$) allowed us to generate long $1ms$ trajectories over 10^9 steps. We analyzed the average position $\langle R(t) \rangle$ and two-point correlation function $\langle R(t)R(0) \rangle$, obtained from simulations, and have compared these quantities with their exact counterparts [13, 14], $\langle R(t) \rangle = R_i(0)\exp[-t/\tau]$ and $\langle R(t)R(0) \rangle = (k_B T/k_{sp})\exp[-t/\tau]$, respectively, where $\tau = \xi/k_{sp}$ is the characteristic time. All RNGs describe well the exact Brownian dynamics except for LCG (Fig. 4). Both $\langle R(t) \rangle$ and $\langle R(t)R(0) \rangle$, obtained using Ran2, Hybrid Taus, and Lagged Fibonacci, practically collapse on the theoretical curve of these quantities. By contrast, using LCG results in repeated patterns of $\langle R(t) \rangle$ and unphysical correlations in $\langle R(t)R(0) \rangle$ (Fig. 4). At longer times, $\langle R(t) \rangle$ and $\langle R(t)R(0) \rangle$, obtained from simulations, deviate somewhat from the theoretical curves due to a soft harmonic spring and insufficient sampling (Fig. 4).

In biomolecular simulations on a GPU, a large memory area should be allocated to store parameters of the force field, Verlet lists, interparticle distances, etc., and the memory demand

scales with the system size as $\sim N^2$. In contemporary graphics cards, the amount of global memory is low, and each memory access takes ~ 300 clock cycles. The number of memory calls scales linearly with the amount of random numbers produced. Because the computational speed even of a fast RNG is determined mostly by the number of global memory calls, multiple reads and writes from and to the GPU global memory can prolong significantly the computational time. We profiled the LCG, and the Ran2, Hybrid Taus, and Lagged Fibonacci RNGs in terms of the number of global memory calls per simulation step. These generators use, respectively, 1, 40, 4, and ~ 3 random seeds per thread (the state size for Lagged Fibonacci depends on the choice of parameters ll and sl). In our implementation, the LCG, and the Hybrid Taus and Lagged Fibonacci RNGs use 4–16 bytes of memory per thread, which is quite reasonable even for large system size $N=10^6$. However, Ran2 requires 280 bytes per thread which is significant for a large system (Table II). Ran2 has large state size, and saving and updating its current state using the GPU local or shared memory is not efficient computationally. Ran2 uses long 64-bit variables, which doubles the amount of data, and requires 4 read and 4 write calls (7 read and 7 write memory calls are needed to generate 4 random numbers). The Hybrid Taus RNG uses the GPU global memory only when it is initialized, and when it updates its current state. Since it uses 4 state variables, 4 read and 4 write memory calls per thread are required irrespectively of the amount of random numbers (Table II). The Lagged Fibonacci RNG uses 2 random seeds, which results in 2 read and 1 write memory calls per random number, and 8 read and 4 write calls for four random numbers (Table II).

To benchmark the computational efficiency of the LCG, and the Ran2, Hybrid Taus, and Lagged Fibonacci RNGs, we carried out LD simulations of N three-dimensional harmonic oscillators in a stochastic thermostat. For each N , we generated one simulation run over $n=10^3$ steps. All N threads have been synchronized at the end of each step to emulate an LD simulation run of a biomolecule on a GPU. The execution time and memory usage are displayed in Fig. 5. Ran2 is the most demanding generator: the use of Ran2 in LD simulations of a system of 10^4 particles adds extra ~ 264 hours of wall-clock time to generate a single trajectory over 10^9 steps (on NVIDIA GeForce GTX 295 graphics card). The memory demand for Ran2 is quite high ($>250MB$ for $N=10^6$). In addition, implementing Ran2 on the GPU does not lead to a substantial speedup compared to the CPU-based implementation (Fig. 5). By contrast, the Hybrid Taus, and Lagged Fibonacci RNGs perform almost equally well in terms of the computational time and memory usage (Fig. 5). These generators require a small amount of memory ($<15-20MB$) even for a large system of 10^6 particles (data not shown).

V. DISCUSSION AND CONCLUSION

Increasing the computational speed of a single CPU core becomes more and more challenging for CPU manufacturers. With accelerated working frequency of modern CPUs, high power throughput results in CPU overheating, which prohibits unlimited growth in their computational power. In this regard, graphics processors are emerging as an alternative type of computing devices that evolve through increasing the number of computational cores rather than working frequency of a few cores. The highly parallel architecture of the GPU device provides an alternative computational platform that allows one to utilize multiple ALUs on a single processor. However, this comes at a price of having smaller cache memory and reduced flow control. Hence, to harvest raw computational power offered by the GPU in a particular application, one has to re-design computational algorithms that have been used on the CPU for several decades. The programmer has to be able to decompose each computational task into many independent threads of execution. In addition, care has to be taken to ensure coalescent memory access, and proper threads synchronization and communication.

Random number generators (RNGs) are needed for most of computer applications such as simulations of stochastic systems, probabilistic algorithms, and numerical analysis among others. We described the one-RNG-per-thread approach and the one-RNG-for-all-threads approach for random number generation on the GPU (Fig. 1), which we applied to the LCG, and to the Ran2, Hybrid Taus, and Lagged Fibonacci generators. We have tested these RNGs using Langevin simulations of N independent Brownian particles, evolving on the harmonic potential. The LCG, Hybrid Taus, and Ran2 algorithms were realized on the GPU as independent RNGs producing many streams of random numbers at the same time (one-RNG-per-thread approach, Fig. 2). Additive Lagged Fibonacci algorithm was implemented using many threads generating a single sequence of random numbers (one-RNG-for-all-threads approach, Fig. 3). The Hybrid Taus and Lagged Fibonacci algorithms of good statistical quality [15, 20, 31] provide random numbers at a computational speed almost equal to that of the Quick and Dirty LCG (Fig. 4), and the associated memory demand is rather low (Figs. 5). Their long periods are sufficient to describe stochastic dynamics of a very large system ($N > 10^6$ particles) on a long timescale ($n > 10^9$ simulation steps). This makes the Hybrid Taus and Lagged Fibonacci algorithms a very attractive option for molecular simulations of biomolecules on the GPU. Ran2 is a well tested generator of proven statistical quality (Fig. 4) [19]. It is probably the best RNG choice for molecular simulations on the CPU, but it works almost ten-fold slower on the GPU and requires large memory area (Fig. 5). Because using Ran2 in the molecular simulations of large systems

can decrease significantly the computational speed of numerical modeling, Ran2 can be used in the simulations of small systems ($N \leq 10^3$ particles).

Statistical characteristics of random numbers, generated by using the one-RNG-per-thread approach, do not improve with the increasing system size. In this setting, each RNG working in each thread uses its own state and, hence, increasing the number of threads (number of particles N) results in the increased number of generators, but it does not improve their statistical qualities. In the one-RNG-for-all-threads approach, streams of random numbers are produced in many threads running in parallel and sharing the same state variables. As a result, statistical properties of the random numbers improve with the increasing size of the RNG state. This is a general property of RNG implementation based on the one-RNG-for-all-threads approach [15, 31]. For this reason, we recommend the Lagged Fibonacci RNG for compute-intensive LD simulations and MD simulations in implicit solvent of large biomolecules, and in parallel tempering algorithms including variants of the replica exchange method. Also, in the one-RNG-for-all-threads approach only one sequence on random numbers is generated, which makes it possible to compare directly the results of simulations on the CPU and on the GPU. This can be used in benchmark tests to estimate numerical errors due to single precision floating point arithmetic, rounding-off errors, or to identify bad memory reads on the GPU.

Profiling the computational performance of the Hybrid Taus and Lagged Fibonacci generators have revealed that for these RNGs the execution time scales sublinearly with N (i.e. remains roughly constant) for $N < 5 \times 10^3$ due to insufficient parallelization, but grows linearly with N for larger systems when all ALUs on the GPU become fully loaded (Fig. 6). Analysis of the execution time for Hybrid Taus and Lagged Fibonacci (RNG time) with the time of generation of deterministic dynamics, i.e. without the Gaussian random forces (dynamics without RNG time), shows that it takes slightly longer to generate random numbers than to propagate the dynamics to the next time step (Fig. 6). This is a pretty high performance level rendering the fact that the potential energy function used in our model simulations does not involve long-range interactions (Lennard-Jones type potential). Using the Hybrid Taus and Lagged Fibonacci RNG leads to a substantial 25–35-fold speedup, as compared to the CPU-based implementation of these generators within the same LD algorithm. Given higher statistical quality of the Hybrid Taus and Lagged Fibonacci RNGs, these generators is a reasonable choice for the GPU-based implementations of molecular simulations (Fig. 5). Hybrid Taus allows one to obtain faster acceleration, compared to Lagged Fibonacci, but the latter has an important advantage over the former, namely, that it can be ported to new graphics cards that utilize Multiple Instruction Multiple Data (MIMD) architecture [44]. We also applied stringent statistical tests of random-

ness to access the statistical properties of random numbers produced by using our GPU-based implementation of the Lagged Fibonacci RNG. We found that even when a small short lag $sl=1252$ is used, this RNG does not fail a single tests in the DIEHARD test suite [25], and passes the BigCrush battery of tests in the TestUO1 package [15].

In conclusion, the development of new Fermi architecture (NVIDIA) [44] and Larrabee architecture (Intel) [45], both equipped with 512 ALUs, is an important next step for general purpose GPU computing. These next generation processors will utilize MIMD protocol, which will enable a developer to use many ALUs in independent computations so that different cores can perform concurrently different computational procedures on multiple data sets. Also, high speed interconnection network will provide a fast interface for threads communication. These advances in computer architecture will enable the programmer to distribute a computational workload among many cores on the GPU more efficiently, and to reach an even higher performance level. In a context of MD simulations in implicit solvent and in LD simulations, it will become possible to compute random forces using much needed threads synchronization over the entire processor. This makes the one-RNG-for-all-threads approach, where thread synchronization is utilized, all the more relevant as it will allow one to obtain additional acceleration on the GPU device gaining from high speed threads communication. Importantly, the GPU-based implementation of the Lagged Fibonacci RNG, developed here, could be ported to new graphics processors with a few minor modifications. In addition, the one-RNG-for-all-threads approach to random number generation can also be used to develop GPU-based implementations of the Mersenne Twister RNG, one of the most revered generators [46–48], and several other generators, including multiple recursive (MRG) and linear/generalized shift feedback register (LSFR/GSFR) generators, such as 4-lag Lagged Fibonacci algorithm [15, 32]. Work in this direction is in progress.

Acknowledgements: Acknowledgement is made to the donors of the American Chemical Society Petroleum Research Fund (grant PRF #47624–G6) for partial support of this research (VB). This work was also supported in part by the grant (#09–0712132) from the Russian Foundation for Basic Research (VB, YK and AZ).

Appendix A: One-RNG-per-thread approach: Hybrid Taus and Ran2

In the pseudocodes, that describe the GPU-based implementation of Hybrid Taus and Ran2 RNGs, superscript h is used to denote the host (CPU) memory, whereas superscript d indicates data stored in the device (GPU) global memory. Also, a section of the code executed on the GPU

is in the same listing as the code for the CPU. In CUDA implementations, the corresponding code for the GPU device is in a separate kernel.

Algorithm 1: Hybrid Taus algorithm.

Require: $y_1^h[N]$, $y_2^h[N]$, $y_3^h[N]$ and $y_4^h[N]$ allocated in CPU memory

Require: $y_1^d[N]$, $y_2^d[N]$, $y_3^d[N]$ and $y_4^d[N]$ allocated in GPU global memory

1. $y_1^h[1 \dots N]$ to $y_4^h[1 \dots N] \leftarrow$ initial seeds
2. $y_1^h[1 \dots N]$ to $y_4^h[1 \dots N] \rightarrow y_1^d[1 \dots N]$ to $y_4^d[1 \dots N]$ {copying initial seeds to GPU}

Beginning of GPU code section

3. $j_{th} \leftarrow$ thread index
4. y_1, y_2, y_3 and $y_4 \leftarrow y_1^d[j_{th}], y_2^d[j_{th}], y_3^d[j_{th}]$ and $y_4^d[j_{th}]$ {loading the state}
5. **for** $i = 1$ to 4; $i++$ **do** {generating four random numbers}
 6. $b \leftarrow (((y_1 \ll c_{11}) \text{ XOR } y_1) \gg c_{21})$
 7. $y_1 \leftarrow (((y_1 \text{ AND } c_1) \ll c_{31}) \text{ XOR } b)$
 8. $b \leftarrow (((y_2 \ll c_{12}) \text{ XOR } y_2) \gg c_{22})$
 9. $y_2 \leftarrow (((y_2 \text{ AND } c_2) \ll c_{32}) \text{ XOR } b)$
 10. $b \leftarrow (((y_3 \ll c_{13}) \text{ XOR } y_3) \gg c_{23})$
 11. $y_3 \leftarrow (((y_3 \text{ AND } c_3) \ll c_{33}) \text{ XOR } b)$
 12. $y_4 \leftarrow ay_4 + c$
 13. Output $mult \times (\text{ XOR } y_1 \text{ XOR } y_2 \text{ XOR } y_3 \text{ XOR } y_4)$
14. **end for**{generating next random number}
15. y_1, y_2, y_3 and $y_4 \rightarrow y_1^d[j_{th}], y_2^d[j_{th}], y_3^d[j_{th}]$ and $y_4^d[j_{th}]$ {saving the current state}

End of GPU code section

In this listing, b is a temporary unsigned integer variable, y_1, y_2, y_3 , and y_4 are unsigned integer random seeds for three Tausworthe generators (lines 6–11) and one LCG (line 12). XOR is a binary operation of exclusive disjunction and “ \gg ” and “ \ll ” denote binary shift to the right and to the left, respectively. In the pseudocode, $mult=2.3283064365387 \times 10^{-10}$ is a multiplier that converts a resulting integer into a floating point number, $c_{11}=13$, $c_{21}=19$, $c_{31}=12$, $c_{21}=2$, $c_{22}=25$, $c_{23}=4$, $c_{31}=3$, $c_{32}=11$, $c_{33}=17$, $c_1=4294967294$, $c_2 = 4294967288$, and $c_3=4294967280$ are constant parameters for three Tausworthe generators [29], and $a=1664525$ and $c=1013904223$ are constant parameters for the LCG [19].

Algorithm 2: Ran2 algorithm.

Require: $idum^h[N]$, $idum2^h[N]$, $iy^h[N]$ and $iv^h[N * NTAB]$ allocated in CPU memory

Require: $idum^d[N]$, $idum2^d[N]$, $iy^d[N]$ and $iv^d[N * NTAB]$ allocated in GPU global memory

1. $idum^h[1 \dots N] \leftarrow$ initial seeds
2. **for** $i = 0$ to $N - 1$; $i ++$ **do** {loading all N generators}
3. $idum2^h[i] \leftarrow idum^h[i]$
4. **for** $j = NTAB + 7$ to 0 ; $j --$ **do**
5. $k \leftarrow idum^h[i]/IQ1$
6. $idum^h[i] \leftarrow IA * (idum^h[i] - k * IQ1) - k * IR1$
7. **if** $idum^h[i] < 0$ **then**
8. $idum^h[i] = idum^h[i] + IM1$
9. **end if**
10. **if** $j < NTAB$ **then**
11. $iv^h[i * NTAB + j] = idum^h[i]$
12. **end if**
13. **end for**
14. **end for**{all N generators are intialized}
15. $idum^h \rightarrow idum^d$; $idum2^h \rightarrow idum2^d$; $iy^h \rightarrow iy^d$; $iv^h \rightarrow iv^d$ {copying to GPU}
16. **for** $t = 0$ to S ; $t ++$ **do** {starting simulation for S steps}

Beginning of GPU code section

17. $j_{th} \leftarrow$ thread index
18. $idum \leftarrow idum^d[j_{th}]$; $idum2 \leftarrow idum2^d[j_{th}]$; $iy \leftarrow iy^d[j_{th}]$ {copying to GPU local memory}
19. $x[4]$ {output vector for four random numbers}
20. **for** $i = 0$ to 4 ; $i ++$ **do** {generating four random numbers}
21. $k \leftarrow idum/IQ1$; $idum \leftarrow IA1 * (idum - k * IQ1) - k * IR1$
22. **if** $idum < 0$ **then**
23. $idum = idum + IM1$
24. **end if**
25. $k \leftarrow idum2/IQ2$; $idum2 \leftarrow IA2 * (idum2 - k * IQ2) - k * IR2$
26. **if** $idum2 < 0$ **then**
27. $idum2 = idum2 + IM2$
28. **end if**
29. $j \leftarrow iy/NDIV$
30. $iv \leftarrow iv^d[j_{th} * NTAB + j]$ {portion of the RNG state in GPU global memory}
31. $iy = iv - idum2$; $idum \rightarrow iv^d[j_{th} * NTAB + j]$
32. **if** $iy < 1$ **then**

```

33.          $iy \leftarrow iy + IMM1$ 
34.     end if
35.      $tempran \leftarrow AM * iy$ 
36.     if  $tempran > RNMX$  then
37.          $x[i] \leftarrow RNMX$ 
38.     else
39.          $x[i] \leftarrow tempran$ 
40.     end if
41. end for{generating next random number}
42.  $idum \rightarrow idum^d[j_{th}]$ ;  $idum2 \rightarrow idum2^d[j_{th}]$ ;  $iy \rightarrow iy^d[j_{th}]$  {saving to GPU global mem-
    ory}
43. Output:  $x$ 

```

End of GPU code section

```

44. end for{next simulation step}

```

Once N RNGs are initialized on the CPU (lines 1–14), initial seeds for all generators are copied to the GPU global memory (line 15). The GPU-based computations start on line 16. Each thread locates the values of the RNG state in the GPU global memory using thread index and copies the values of variables $idum$, $idum2$ and iy to the GPU local memory (line 18). Array iv is accessed via GPU global memory calls (lines 30 and 31). Each thread generates four random numbers (cycle starting on line 20) and saves them to array $x[4]$. Current RNG state variables are updated in the GPU global memory (line 42).

Appendix B: One-RNG-for-all-threads approach: Lagged Fibonacci

Algorithm 3: Additive Lagged Fibonacci algorithm.

Require: $x^d[N]$ allocated in GPU global memory

1. $x^d[1 \dots ll] \leftarrow$ initial seeds
2. **for** $t = 0$ to S **do** {starting simulations}

Beginning of GPU code section

3. $j_{th} \leftarrow$ thread index
4. $shift_0 \leftarrow (j_{th} + N * t) * RNS$
5. **for** $shift = shift_0$ to $shift_0 + RNS - 1$ **do**
6. $x_{ll} \leftarrow x^d[shift \bmod ll]$
7. $x_{sl} \leftarrow x^d[(shift + sl - ll) \bmod ll]$

```

8.          $x \leftarrow (x_{ll} \text{ op } x_{sl}) \bmod m$ 
9.         output  $x$ 
10.         $x \rightarrow x^d[\text{shift} \bmod ll]$ 
11.    end for

```

End of GPU code section

```
12. end for
```

To initialize a RNG, a CPU fills in ll integer random seeds into x^d arrays and copies them to the GPU (line 1), where each thread computes the location (*shift0*) of an integer that corresponds to the location of the first random number to be produced. This is done using the current simulation step (t), thread index (jth), the total number of threads (N), and the amount of random numbers needed at each step (RNS). Lines 6–10 are repeated until RNS random numbers are generated (cycle starting on line 5) using addition operator *op* (line 8). For every random number, two integers from the RNG state have to be gathered (lines 6 and 7). These integers correspond to the long lag ll and the short lag sl . Locations in the array of integers are modulo ll , which represents “cycling” through the array of state integers starting from the beginning of the array (when its end is reached). The resulting integer x (line 8) is reported (line 9) and saved for the next steps (line 10). When RNS random numbers are needed in each thread at each step of a simulation, $sl > RNS \times N$ and $ll - sl > RNS \times N$ (total number of integers updated at each step is $RNS \times N$).

-
- [1] J. E. Stone, J. C. Phillips, P. L. Freddolino, D. J. Hardy, L. G. Trabuco, and K. Schulten, “Accelerating molecular modeling applications with graphical processors,” *J. Comput. Chem.*, vol. 28, pp. 2618–2640, 2007.
 - [2] M. S. Friedrichs, P. Eastman, V. Vaidyanathan, M. Houston, S. Legrand, A. L. Beberg, D. L. Ensign, C. M. Bruins, and V. S. Pande, “Accelerating molecular dynamic simulation on graphics processing units,” *J. Comput. Chem.*, vol. 30, pp. 864–872, 2009.
 - [3] J. A. Anderson, C. D. Lorentz, and A. Travesset, “General purpose molecular dynamics simulations fully implemented on graphics processing units,” *J. Comput. Phys.*, vol. 227, pp. 5342–5359, 2008.
 - [4] J. A. van Meel, A. Arnold, D. Frenkel, S. F. P. Zwart, and R. Belleman, “Harvesting graphics power for MD simulations,” *Mol. Simul.*, vol. 34, no. 3, pp. 259–266, 2008.
 - [5] M. J. Harvey and G. D. Fabritius, “An implementation of the smooth Particle Mesh Ewald method on GPU hardware,” *J. Chem. Theory Comput.*, vol. 5, pp. 2371–2377, 2009.

- [6] J. E. Davis, A. Ozsoy, S. Patel, and M. Taufer, “Towards large-scale molecular dynamics simulations on graphics processors,” in *BICoB '09: Proceedings of the 1st International Conference on Bioinformatics and Computational Biology*, (Berlin, Heidelberg), pp. 176–186, Springer-Verlag, 2009.
- [7] A. G. Anderson, W. A. G. III, and P. Schröder, “Quantum Monte Carlo on graphical processing units,” *Comput. Phys. Commun.*, vol. 177, pp. 298–306, 2007.
- [8] J. Yang, Y. Wang, and Y. Chen, “GPU accelerated molecular dynamics simulations of thermal conductivities,” *J. Comput. Phys.*, vol. 221, pp. 799–804, 2007.
- [9] NVIDIA, *NVIDIA CUDA Programming Guide*, 2.3.1 ed., 2009.
- [10] NVIDIA, *NVIDIA CUDA C Programming Best Practices Guide*, 2.3 ed., July 2009.
- [11] B. R. Brooks, R. E. Bruccoleri, B. D. Olafson, D. J. States, S. Swaminathan, and M. Karplus, “CHARMM: A program for macromolecular energy, minimization, and dynamics calculations,” *J. Comput. Chem.*, vol. 4, no. 2, pp. 187–217, 1983.
- [12] U. Haberthür and A. Caffisch, “FACTS: Fast analytical continuum treatment of solvation,” *J. Comput. Chem.*, vol. 29, no. 5, pp. 701–715, 2008.
- [13] H. Risken, *The Fokker-Planck Equation*. Springer-Verlag, second ed., 1989.
- [14] M. Doi and S. Edwards, *The Theory of Polymer Dynamics*. International Series of Monographs on Physics, Oxford Science Publications, 1988.
- [15] P. L’Ecuyer and R. Simard, “TestU01: A C library for empirical testing of random number generators,” *ACM Trans. Math. Softw.*, vol. 33, no. 4, p. 22, 2007.
- [16] W. W. Tsang and G. Marsaglia, “The Ziggurat method for generating random variables,” *J. Stat. Softw.*, vol. 5, no. 08, 2000.
- [17] G. Marsaglia and T. A. Bray, “A convenient method for generating normal variables,” *SIAM Rev.*, vol. 6, no. 3, pp. 260–264, 1964.
- [18] G. E. P. Box and M. E. Miller, “A note on the generation of normal random deviates,” *Ann. Math. Statist.*, vol. 29, pp. 610–611, 1958.
- [19] W. H. Press, S. A. Teukolsky, W. T. Vetterling, and B. P. Flannery, *Numerical Recipes in C. The Art of Scientific Computing*, Cambridge University Press, second ed., 1992.
- [20] H. Nguyen, ed., *GPU Gems 3*. Addison-Wesley, 2008.
- [21] L. Barreira, “Poincaré recurrence: old and new,” in *XIVth International Congress on Mathematical Physics*, pp. 415–422, World Scientific, 2006.
- [22] W. Selke, A. L. Talapov, and L. N. Shchur, “Cluster-flipping Monte Carlo algorithm and correla-

- tions in “good” random number generators,” *JETP Lett.*, vol. 58, no. 8, pp. 665–668, 1993.
- [23] P. Grassberger, “On correlations in “good” random number generators,” *Phys. Lett. A*, vol. 181, no. 1, pp. 43–46, 1993.
- [24] A. M. Ferrenberg, D. P. Landau, and Y. J. Wong, “Monte Carlo simulations: Hidden errors from “good” random number generators,” *Phys. Rev. Lett.*, vol. 69, no. 23, pp. 3382–3384, 1992.
- [25] G. Marsaglia, “DIEHARD: A battery of tests of randomness,” 1996. Available at: <http://stat.fsu.edu/geo/diehard.html>.
- [26] M. Mascagni and A. Srinivasan, “Algorithm 806: SPRNG: A scalable library for pseudorandom number generation,” *ACM Trans. Math. Softw.*, vol. 26, pp. 436–461, 2000.
- [27] J. Soto, “Statistical testing of random number generators,” 1999. Available at: <http://csrc.nist.gov/rng/>.
- [28] R. C. Tausworthe, “Random numbers generated by linear recurrence modulo two,” *Math. Comput.*, vol. 19, no. 90, pp. 201–209, 1965.
- [29] P. L’Ecuyer, “Maximally equidistributed combined Tausworthe generators,” *Math. Comput.*, vol. 65, no. 213, pp. 203–213, 1996.
- [30] M. Mascagni and A. Srinivasan, “Parameterizing parallel multiplicative lagged-Fibonacci generators,” *Parallel Comput.*, vol. 30, no. 7, pp. 899–916, 2004.
- [31] R. P. Brent, “Uniform random number generators for supercomputers,” in *Proc. Fifth Australian Supercomputer Conference*, pp. 95–104, 1992.
- [32] G. Marsaglia, “Random numbers for C: The END?.” Published on sci.crypt, 1999.
- [33] R. P. Brent, S. Larvala, and P. Zimmermann, “A fast algorithm for testing reducibility of trinomials mod 2 and some new primitive trinomials of degree 3021377,” *Math. of Comput.*, vol. 72, no. 243, pp. 1443–1452, 2003.
- [34] P. L’Ecuyer, F. Blouin, and R. Couture, “A search for good multiple recursive random number generators,” *ACM Trans. Model. Comput. Simul.*, vol. 3, no. 2, pp. 87–98, 1993.
- [35] D. L. Ermak and J. A. McCammon, “Brownian dynamics with hydrodynamic interactions,” *J. Chem. Phys.*, vol. 69, no. 4, pp. 1352–1360, 1978.
- [36] G. Hummer and A. Szabo, “Kinetics from nonequilibrium single-molecule pulling experiments,” *Biophys. J.*, vol. 85, pp. 5–15, 2003.
- [37] V. Barsegov, D. Klimov, and D. Thirumalai, “Mapping the energy landscape of biomolecules using single molecule force correlation spectroscopy: Theory and applications,” *Biophys. J.*, vol. 90, pp. 3827–3841, 2006.

- [38] M. Mickler, R. I. Dima, H. Dietz, C. Hyeon, D. Thirumalai, and M. Rief, “Revealing the bifurcation in the unfolding pathways of GFP by using single-molecule experiments and simulations,” *Proc. Natl. Acad. Sci. USA*, vol. 104, no. 51, pp. 20268–20273, 2007.
- [39] V. Tozzini, “Coarse-grained models for proteins,” *Curr. Opin. Struct. Biol.*, vol. 15, no. 2, pp. 144–150, 2005.
- [40] C. Clementi, “Coarse-grained models of protein folding: toy models or predictive tools?,” *Curr. Opin. Struct. Biol.*, vol. 18, no. 1, pp. 10–15, 2008.
- [41] C. Hyeon, R. I. Dima, and D. Thirumalai, “Pathways and kinetic barriers in mechanical unfolding and refolding of RNA and proteins,” *Structure*, vol. 14, pp. 1633–1645, 2006.
- [42] R. I. Dima and H. Joshi, “Probing the origin of tubulin rigidity with molecular simulations,” *Proc. Natl. Acad. Sci. USA*, vol. 105, no. 41, pp. 15743–15748, 2008.
- [43] T. Veitshans, D. Klimov, and D. Thirumalai, “Protein folding kinetics: timescales, pathways and energy landscapes in terms of sequence-dependent properties,” *Fold. Des.*, vol. 2, no. 1, pp. 1–22, 1997.
- [44] NVIDIA, *NVIDIA’s Next generation CUDA Compute Architecture: Fermi*, 1.1 ed., 2009.
- [45] L. Seiler, D. Carmean, E. Sprangle, T. Forsyth, M. Abrash, P. Dubey, S. Junkins, A. Lake, J. Sugerman, R. Cavin, R. Espasa, E. Grochowski, T. Juan, and P. Hanrahan, “Larrabee: A many-core x86 architecture for visual computing,” in *SIGGRAPH ’08: ACM SIGGRAPH 2008 papers*, (New York, NY, USA), pp. 1–15, ACM, 2008.
- [46] M. Matsumoto and Y. Kurita, “Twisted GFSR generators,” *ACM Trans. Model. Comput. Simul.*, vol. 2, no. 3, pp. 179–194, 1992.
- [47] M. Matsumoto and Y. Kurita, “Twisted GFSR generators II,” *ACM Trans. Model. Comput. Simul.*, vol. 4, no. 3, pp. 254–266, 1994.
- [48] M. Matsumoto and T. Nishimura, “Mersenne Twister: A 623-dimensionally equidistributed uniform pseudo-random number generator,” *ACM Trans. Model. Comput. Simul.*, vol. 8, no. 1, pp. 3–30, 1998.

FIGURE CAPTIONS

Fig. 1. Flowchart for generation of random numbers using the one-RNG-per-thread approach (panel *a*) and the one-RNG-for-all-threads approach (panel *b*). In the one-RNG-per-thread setting, N independent RNGs (for N particles) are running concurrently in N computational threads on the GPU device generating random numbers from the same sequence, but starting from different sets of initial seeds. Within the one-RNG-for-all-threads approach, a single RNG is used by all N threads running in parallel on the GPU sharing one set of seeds and producing N subsequences of the same sequence of random numbers. The computational workflow is indicated by the arrows, and $n, n + 1, \dots$ are the simulation steps.

Fig. 2. GPU-based realization of the one-RNG-per-thread approach. The arrows represent the direction of computational workflow and data transfer. To launch an RNG on the GPU, N sets of initial random seeds, one set per thread of execution (per particle) generated on the CPU, are transferred to the GPU global memory. Each thread reads corresponding seeds from the GPU global memory, and generates random numbers for just one step of a simulation using a particular RNG algorithm. When all random numbers have been produced at the n -th step, each thread saves its RNG state to the GPU global memory so that it could be used at the next step ($n + 1$).

Fig. 3. GPU-based realization of the one-RNG-for-all-threads approach and parallel implementation of the Lagged Fibonacci algorithm using the cycle division paradigm. The state of the Lagged Fibonacci RNG is represented by the circle of ll integers. Initial seeds are generated on the CPU and copied to the GPU global memory. Generation of N random numbers is done simultaneously in N threads using Eq. (3) (shown by arrows). The obtained random numbers are saved to update the RNG state for future use. A grid of computational threads is moving along the same sequence of random numbers, each time rewriting N state variables that appear ll positions earlier in the sequence. The dark grey squares represent the state variables, and the updated portion of the RNG state at a given step; the black “zero line”, which denotes the position of the first thread, shifts forward by N positions at every next step.

Fig. 4. Semilogarithmic plots of the average particle position $\langle X(t) \rangle$ (panels *a* and *b*) and two-point correlation function $C(t) = \langle X(t)X(0) \rangle$ (panel *c*) for a system of N harmonic oscillators in a stochastic thermostat. Theoretical curves of $\langle X(t) \rangle$ and $C(t)$ are compared with the results of Langevin simulations obtained using the LCG, Hybrid Taus, Ran2, and Lagged Fibonacci algorithms. Equilibrium fluctuations of $\langle X(t) \rangle$ on a longer timescale, obtained using LCG,

are magnified in panel *b*, where one can observe a repeating pattern due to the inter-stream correlations among N streams of random numbers.

Fig. 5. Computational performance of the GPU-based implementations of the LCG, Ran2, Hybrid Taus, and Lagged Fibonacci algorithms in LD simulations of N three-dimensional harmonic oscillators in a stochastic thermostat (color code is explained in the graphs). Panel *a*: A logarithmic plot of the execution time (per 10^3 steps) as a function of the system size N . Threads have been synchronized on the CPU at the end of each step to imitate the LD simulations of a biomolecule. As a reference, also shown is the simulation time with the Ran2 algorithm implemented on the CPU. Panel *b*: Memory demand, i.e. the amount of memory needed for an RNG to store its current state, as a function of N . A step-wise increase in the memory usage for Lagged Fibonacci at $N \approx 0.6 \times 10^5$ is due to change in the values of constant parameters (Table I).

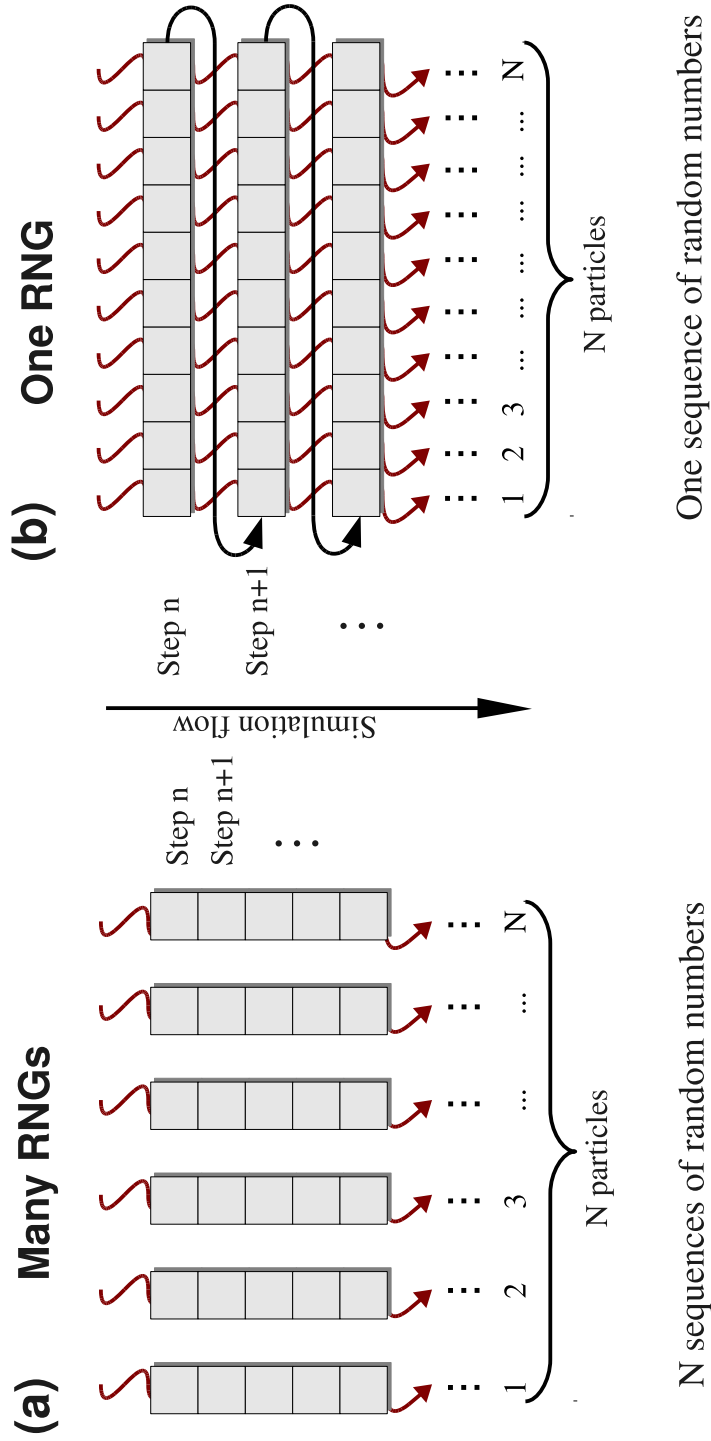
Fig. 6. Computational time (per 10^3 steps) for an end to end application of LD simulations of N three-dimensional harmonic oscillators in a stochastic thermostat using the Hybrid Taus (panel *a*) and Lagged Fibonacci algorithm (panel *b*), as a function of N (color code is explained in the graphs). The simulation time for the full LD algorithm (Langevin Dynamics) is compared with the time for generating random numbers (RNG) and with the time required to obtain deterministic dynamics without random numbers (Dynamics w/o RNG). The computational speedup (CPU time/GPU time) is displayed in the insets.

TABLE I: Constant parameters, i.e. the short lag sl and the long lag ll , for the Lagged Fibonacci RNG for molecular simulations of a system of size N (taken from Ref. [31, 33]).

N	<1252	<3004	<5502	<10095	<12470	<23463	<54454	<279695	<288477	<1010202
sl	1 252	3 004	5 502	10 095	12 470	23 463	54 454	279 695	288 477	1 010 202
ll	2 281	4 423	9 689	19 937	23 209	44 497	132 049	756 839	859 433	3 021 377

TABLE II: Memory usage (in bytes/thread), and the number of GPU global memory calls, i.e. the numbers of read/write operations per one random number (M_1) and for four random numbers (M_2), for generation of random numbers on the GPU at each step using the LCG, and the Hybrid Taus, Ran2, and Lagged Fibonacci RNGs. In molecular simulations, four random numbers are needed at each step to generate three (x , y , and z) components of the Gaussian random force per particle.

Parameter	LCG	Hybrid Taus	Ran2	Lagged Fibonacci
bytes/thread	4	16	280	12
M_1	1/1	4/4	4/4	3/1
M_2	1/1	4/4	7/7	12/4



One sequence of random numbers

N sequences of random numbers

Figure 1. (A. Zhmurov, K. Rybnikov, Y. Kholodov, V. Barsegov)

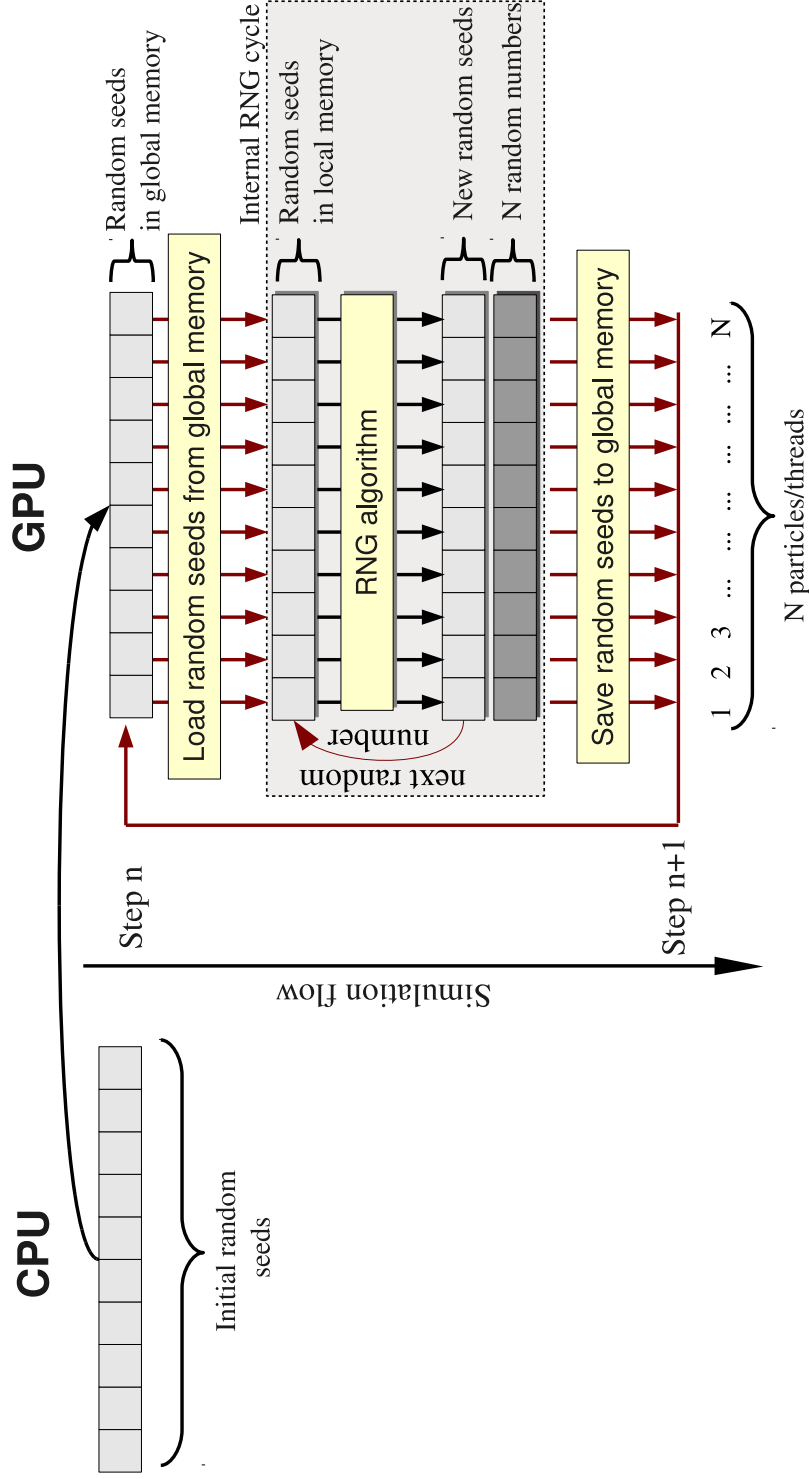


Figure 2. (A. Zhmurov, K. Rybnikov, Y. Kholodov, V. Barsegov)

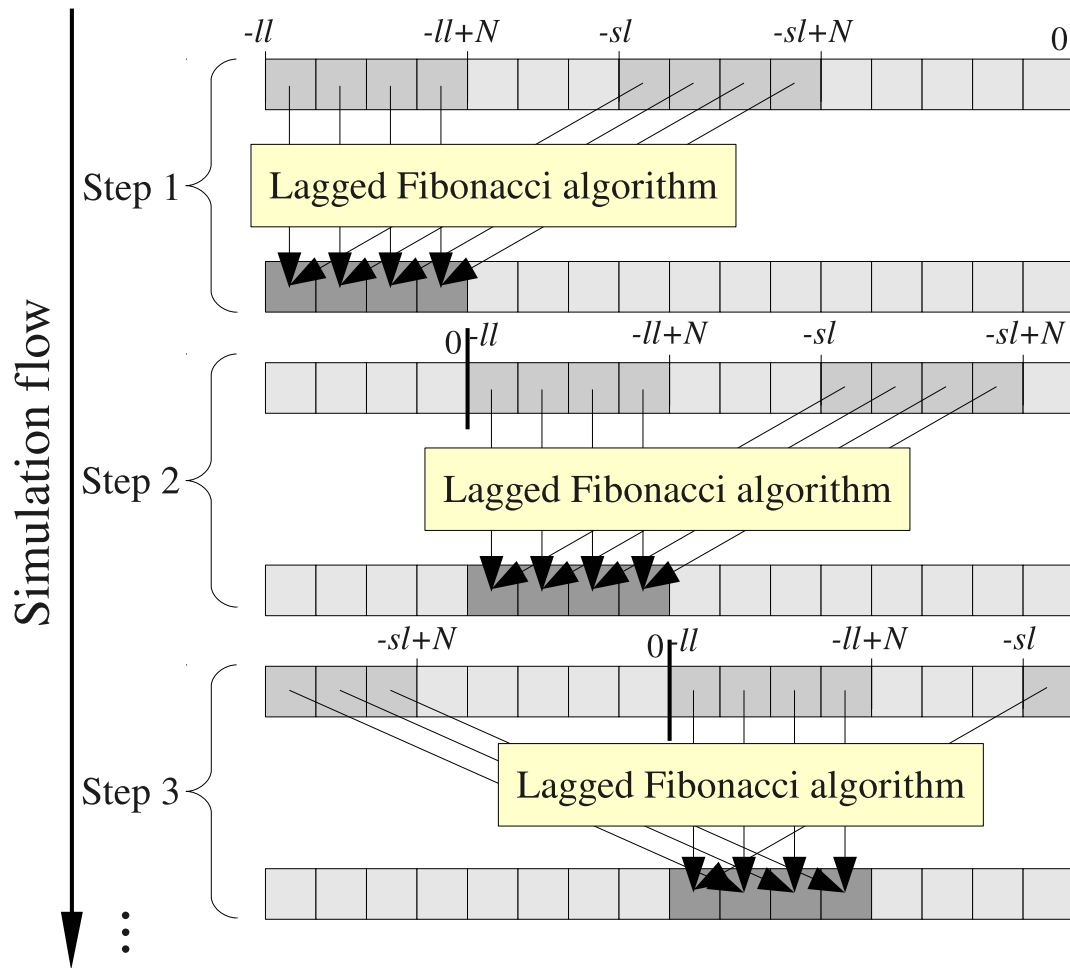


Figure 3. (A. Zhmurov, K. Rybnikov, Y. Kholodov, V. Barsegov)

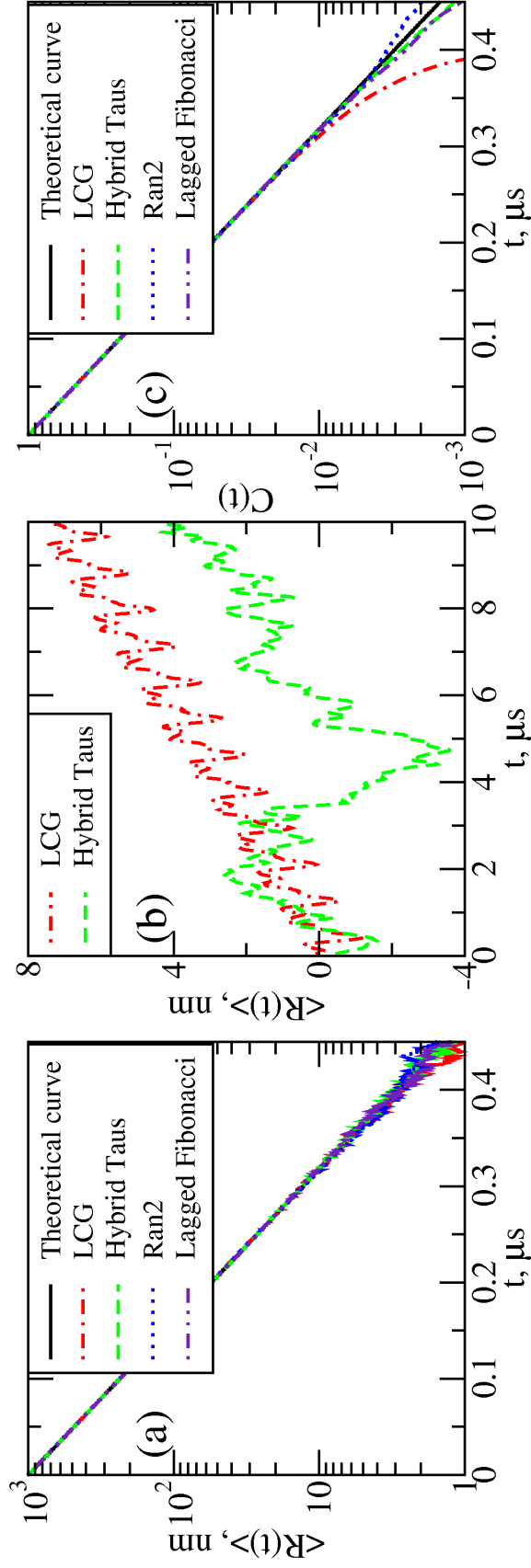


Figure 4. (A. Zhmurov, K. Rybnikov, Y. Kholodov, V. Barsegov)

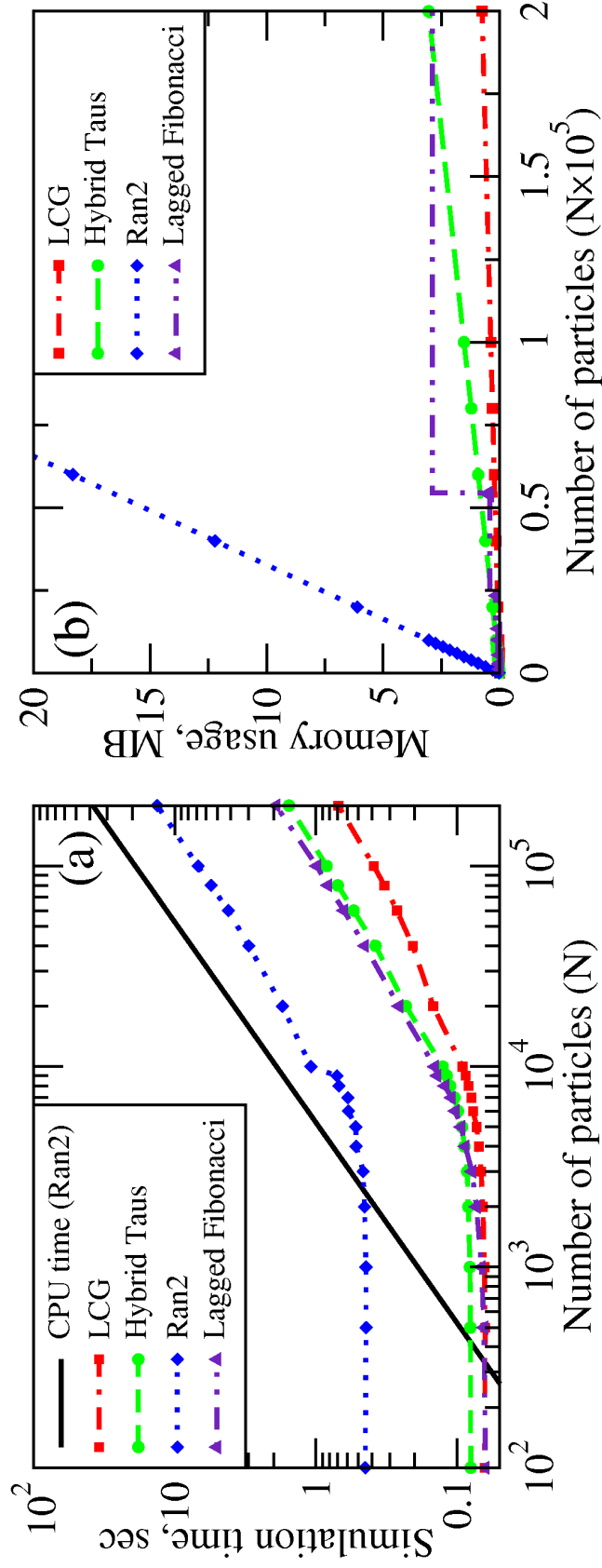


Figure 5. (A. Zhmurov, K. Rybnikov, Y. Kholodov, V. Barsegov)

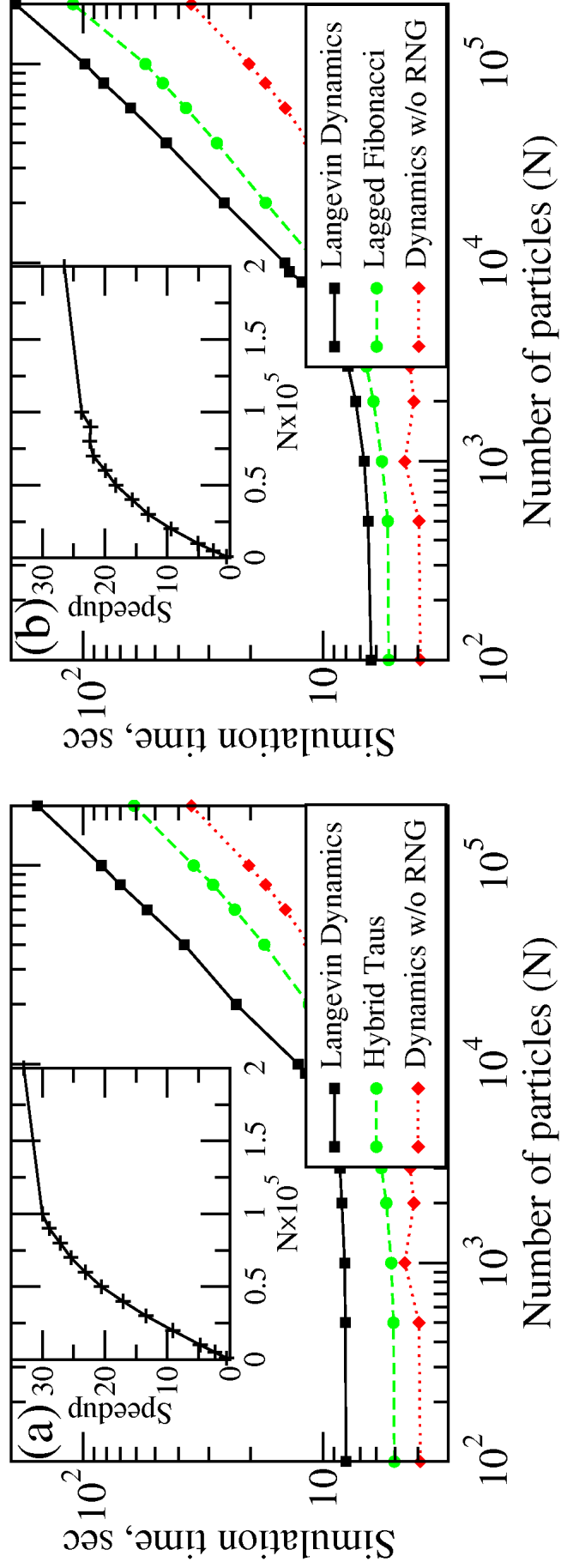


Figure 6. (A. Zhmurov, K. Rybnikov, Y. Kholodov, V. Barsegov)